Multi-Faceted Maximization of a Microgrid-Incorporated Hybrid Photovoltaic-Wind-Battery-Diesel System in Basra, Iraq

Aqeel Mezher Thajeel Alsultan
Faculty of Artificial Intelligence
Universiti Teknologi Malaysia
Kuala Lumpur, Malaysia
mezher@graduate.utm.my

Nurul Aini Bani
Faculty of Artificial Intelligence
Universiti Teknologi Malaysia
Kuala Lumpur, Malaysia
nurulaini.kl@utm.my

Mohd Nabil Muhtazaruddin
Faculty of Artificial Intelligence
Universiti Teknologi Malaysia
Kuala Lumpur, Malaysia
mohdnabil.kl@utm.my

Firdaus Muhammad-Sukki
School of Engineering and Built Environment
Edinburgh Napier University
Edinburgh, United Kingdom
f.muhammadsukki@napier.ac.uk

***Abstract*—Hybrid Renewable Energy Sources (HRES) in microgrids present a cost-effective option for supplying power to remote areas. This research focuses on optimizing HRES systems for Base Transceiver stations in Basra, Iraq, by using the Multiobjective Improve Salp Swarm algorithm (MOISSA) to enhance reliability, reduce energy costs, and improve energy distribution through effective design variables such as photovoltaic power, wind turbines, and battery autonomy days. Through MATLAB simulations with the MOISSA algorithm, and comparative analysis to other algorithms, the study shows a significant reduction in energy costs and a decrease in power supply probability, offering valuable design solutions for Hybrid Microgrid Systems.**

Keywords— hybrid renewable energy sources, multiobjective salp swarm, algorithm, microgrid

I. INTRODUCTION

The increasing global attention towards alternative energy sources is driven by factors like population growth, escalating energy needs, higher production expenses, greenhouse gas emissions, and the environmental effects of fossil fuels. Despite progress in renewable energy technologies, rural areas and islands still struggle with electricity shortages, making wind, solar, and hydropower essential due to their widespread availability, cleanliness, and user-friendly nature [1-4]. The integration of wind and solar power in a hybrid energy system improves reliability and quality, with the option to include storage devices for efficiency during periods of low wind or solar activity, making Hybrid Microgrid Systems (HMS) the most efficient and cost-effective solution for utilizing localized renewable energy sources in off-grid areas, despite the complexity of planning and designing these systems due to economic and technical challenges related to the variability of renewable energy sources and the necessity for optimal sizing and energy management strategies to effectively meet electricity demands [5,6].

Prior studies have explored the sizing of hybrid microgrid systems using different methods. The first category includes software tools like HOMER, HOMER Pro, PVSYST, HOGA, IHOGA, and RAPSIM, but users struggle to choose suitable components intuitively [7-10]. Deterministic strategies make up the second classification, requiring substantial simulation time to evaluate all system configurations. Metaheuristic algorithms form the third category, with Fathy et al. [11] introducing a method using social spider optimizers for microgrid sizing in Saudi Arabia. Bukar et al. applied the grasshopper optimization algorithm in Nigeria, while Farh et al. [12] used the bonobo optimizer in Saudi Arabia to minimize system cost. Jufri et al. [13] optimized a hybrid power generation system in Indonesia, and Borhanazad et al. presented a multi-objective particle swarm optimization technique in Iran [14]. The summary of the literature findings is shown in Table 1.

The study utilizes the novel meta-heuristic optimization algorithm MOISSA to optimize dimensions in hybrid microgrid systems and suggests an Energy Management System, showing superior performance in convergence speed and balancing exploration and exploitation when compared to other algorithms, as detailed in the paper's structured sections focusing on system components, Energy Management Strategy (EMS), optimization results, and result analysis.

TABLE I. SUMMARY OF THE LITERATURE FINDINGS ON HYBRID MICROGRID SYSTEMS.

Reference	**Year**	**Country**	**Objective function**	**Algorithm**
[15]	2021	Saudi Arabia	Reducing the Annual LPSP/COE	Multiobjective Evolutionary Algorithm
[16]	2020	Nigeria	Reducing the Annual COE/DPSP	The Multiobjective Grasshopper

				Optimization Algorithm is a computational method for solving multiple objective optimization problems.
[17]	2022	Saudi Arabia	Reduce the overall Annualized System Cost (ASC) to a minimum.	The Bonobo Optimizer is a method that users use.
[18]	2022	Saudi Arabia	Employed to reduce the Annual COE.	HOMER
[19]	2021	India	Reducing the Annual NPC/COE	HOMER
[11]	2020	Saudi Arabia	Reduce the overall Annualized System Cost (ASC) to a minimum	Utilizing techniques derived from the Social Spider Optimizer algorithm.
[21]	2019	Egypt	Minimizing the Annual LPSP/COE while maximizing RF.	Employing the Multiobjective Dragonfly Algorithm (MODA) methodology
[22]	2020	China	The objective is to reduce the Annual CACS/DPSP	Employing the Multiobjective Grey Wolf Optimizer techniques

II. THE ENERGY MANAGEMENT SYSTEM FOR A HYBRID MICROGRID SYSTEM

The study employs a framework illustrated in Figure 1, including photovoltaic (PV), wind turbine (WT), battery technologies (BT), and diesel generator (DG) elements, to construct Hybrid Renewable Energy Systems (HRES) for sustainable energy generation, utilizing various converters for battery regulation, power management, electricity conversion, and control, alongside an RB-EMS algorithm by Kempener et al. [23] for operational efficiency through hourly data collection on ambient temperature, solar irradiance, SOC, and load profile.

The Energy Management Strategy (EMS) plays a critical role in designing autonomous microgrids by regulating power distribution among system components to enhance efficiency and cost-effectiveness. This study implemented four distinct EMS approaches, including utilizing renewable energy sources, battery storage, and diesel generators to meet load demands and optimize energy conservation benefits. The flow chart of the rule-based EMS is shown in Figure 2.

III. MULTIOBJECTIVE SALP SWARM ALGORITHM

The Salp Swarm Algorithm (SSA) is a unique swarm intelligence method considered a metaheuristic optimization algorithm, inspired by the foraging behaviour and cognitive skills of salps, as introduced by Mirjalili et al. in 2017, where organisms form chains led by a designated leader to collectively search for food, as depicted in Figures 3a and 3b.

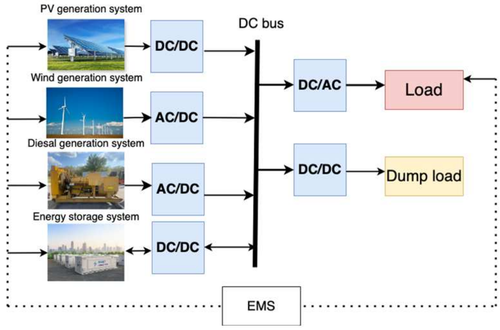

Fig. 1. Layout of an independent microgrid system.

The Improved Salp Swarm Algorithm (ISSA) is an upgraded version of the SSA algorithm, displaying improved precision and optimality, as evidenced in studies by Wang et al. [24] and Duan et al. [25]. It demonstrates rapid computational efficiency, enhanced efficacy, and dependable convergence capabilities, effectively tackling economic dispatch issues, as Balakrishnan et al. highlighted [26]. Differentiations between SSA and ISSA lie in the random process and selection approach, with ISSA employing Levy flight for enhanced effectiveness. The depiction of ISSA can be observed in Figure 4, where Levy flight dictates the model's advancement in size and direction by utilizing the Levy distribution, characterized by a power-law tail probability function [26]. The Mantegna method [25] generates the corresponding numerical value based on the Levy distribution in this research, with the mathematical processes for the proposed algorithm detailed in Equations (1-5).

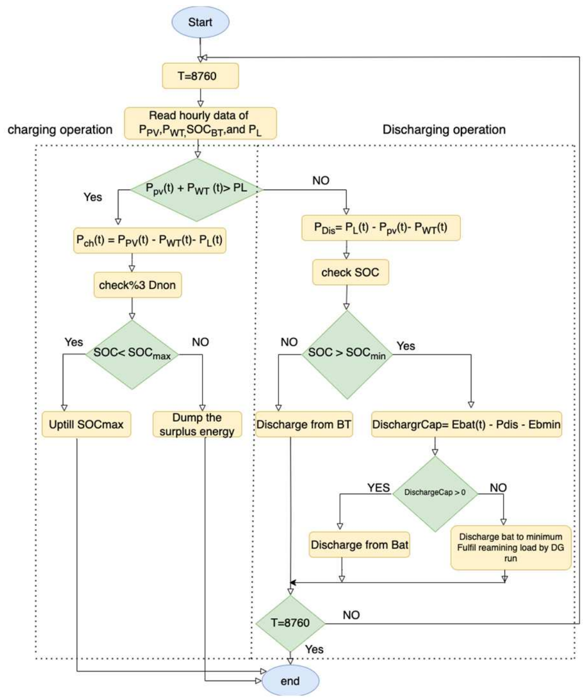

Fig. 2. Flow chart of the rule-based energy management strategy

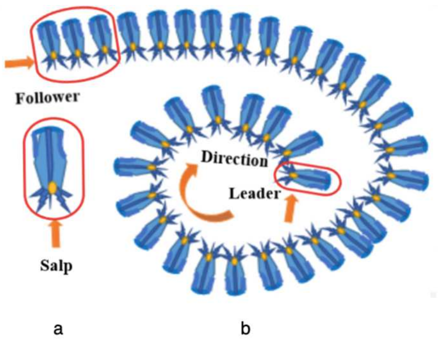

Fig. 3. Illustration of various salp, with (a) symbolizing the dominant salp and (b) showing the chin .

$$levy\ (\propto) = 0.05\ \times \times \frac{m}{|n\,|^{1-\propto}} \quad (1)$$

Where $1 < \alpha \leq 2$, the standard deviation σ_m and σ_n represent the normal distribution of arbitrary numbers m and n, respectively:

$$m = normal\ (0, \sigma_m^2) \quad (2)$$
$$n = nornal\ (0, \sigma_n^2) \quad (3)$$

The value of σ_m in equation (2) is determined through the following calculation:

$$\sigma m = \left[\frac{y(1+\propto) sin\frac{\pi a}{2}}{y\left(\frac{(1+\propto)}{2}\right) \propto 2^{\frac{(\propto-1)}{2}}}\right]^{\frac{1}{\propto}} \quad (4)$$

The use of incremental and intermittent extensive movements in a Levy flight improves the search efficiency of an optimization framework by thoroughly exploring the vicinity of the current optimal solution and potentially covering a wider search space, leading to the successful discovery of the most efficient solution in the initial stage of ISSA, random coordinates are generated for salps based on the input data dimensions, followed by formulating solutions with randomly selected attributes from existing features. In the update phase, the ISSA adjusts the positions of search agents' leaders and followers. In contrast, the ISSA utilizes P_1 Long to update salps' positions with the food source, limiting their convergence range. By introducing randomness through Levy flight to update salps' positions, exploration capabilities are enhanced, preventing them from getting stuck in local optima and promoting foraging, hence expanding the search space explored, as demonstrated by Wang et al. [27].

$$Stepsize = Levy(\propto) \times (S_j - Levy(\propto) \times y_j \quad (5)$$

After determining the appropriate step size, the leader's location is adjusted using equations (3,4).

$$y_j^1 = \begin{cases} Sj + P_1\left((UB_j - LB_j)P_2 + LB_j\right) P_3 \geq 0 \\ S_j - P_1\left((UB_j - LB_j)P_2 + LB_j\right) P_j < 0 \end{cases} \quad (6)$$

$$y_j^1 = y_j^1 + Stepsize_j \quad (7)$$

$$y_j^1 = \frac{1}{3}\left(y_j^i + y_j^{i-1} + Levy(\propto)\right) \quad (8)$$

To enhance the ISSA's exploration capabilities and avoid local optima stagnation, it is recommended that the step size of the initial random solution be increased. MOISSA utilizes various strategies to tackle sizing issues, as depicted in Figure 4, by dispersing random particles within user-defined boundaries to refine the objective function through space traversal. The effectiveness and efficiency of MOISSA were evaluated through experiments comparing its performance with other optimization algorithms like (MOSSA), (MOALO), and (MOPSO), revealing that MOISSA effectively balances exploration and exploitation compared to its counterparts.

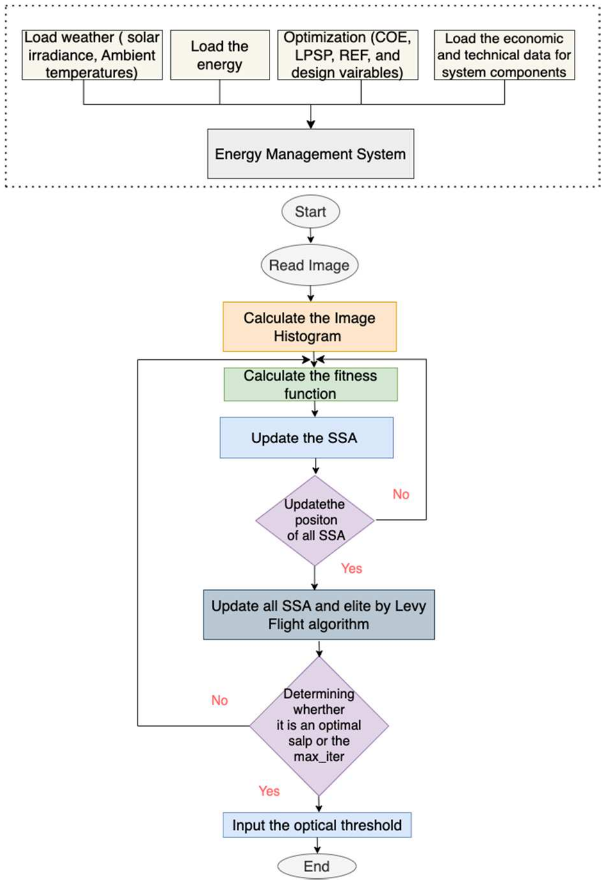

Fig. 4. Flow chart of the Molitobjective Improved Salp Swarm Algorithm (MOISSA).

IV. Results and Discussion

The current study presents various options for the optimal configuration of the analyzed microgrid utilizing a multiobjective optimization technique. This strategy yields a collection of optimal solutions called the Pareto front. MOISSA, MOSSA, MOPSO, and MOALO were subjected to over 100 iterations. The results of utilizing the techniques above for independent microgrid setups exhibit a remarkable and uniform spread. This analysis is conducted based on LPSP and COE functions. The outcomes displayed on the Pareto front reveal not just an optimal solution but also a set of optimal solutions (non-dominated solutions) and a range of potential design decisions. The subsequent section discusses the findings from applying the MOISSA, MOSSA, MOPSO, and MOALO algorithms.

A. Comparative Analysis

The utilization of ISSA in the simulation aimed to decrease both the Cost of Energy (COE) and Loss of Power Supply probability (LPSP). The findings presented in Figure 5 demonstrate that as the limit for LPSP rises, the ASC diminishes. However, achieving 100% reliability necessitates a more substantial diesel generator and increased incorporation of renewable energy, consequently leading to a higher annualized system cost. The evaluation of the performance of the four algorithms concerning the Pareto front is depicted in Fig 5, revealing that ISSA exhibits comparable and superior performance compared to SSA, PSO, and ALO.

This paper presents diverse options for the most suitable configuration of the analyzed load BTS using a multi-objective optimization strategy. This strategy generates a collection of optimal solutions called the Pareto front. Within multi-objective decision-making, identifying a solution from the Pareto front is crucial. The Pareto front encompasses a set of solutions not dominated by others. Optimal solutions are chosen from this collection, which can be likened to a Cartesian graph, where the x-axis value is the sole variable used to determine a solution. It is essential to define a specific variable, such as LPSP = 0%, LPSP = 1%, LPSP = 2%, etc., to achieve a solution. This method serves two main purposes: first, it illustrates the impact of cost variation with different LPSP values at 1%, 2%, and 3%, and second, it demonstrates how adjustments to the aforementioned variable influence design.

Table compares all four algorithms utilizing a Pareto front solution. The cost of energy for ISSA, PSO, SSA, and ALO are 0.1521, 0.1552, 0.1538, and 0.1530 $/kWh, respectively. If we compare all four algorithms based on the cost of energy production, ISSA produces energy at the lowest price of 0.1521$ per unit. The system is modelled to operate using entirely dependable renewable energy sources. The annualized expenditure for the system amounts to 89171.83$. By allowing the LPSP threshold to reach 5%, the annualized cost of the system decreases to 63322.34$. Likewise, when the LPSP threshold is set at 10%, the annualized cost of the system is 51382.18$, and at 20% LPSP, the system cost further drops to 42683.69$. A solution is chosen from the Pareto front where a 5% loss of power supply probability is accepted. This final solution includes an 87.04kW wind turbine, a 9.48kW solar system, a 76.07 kWh battery storage system, and a 20.42kW diesel generator. The annualized cost of this system remains at 89171.83$, with an energy production cost of 0.152$/kW.

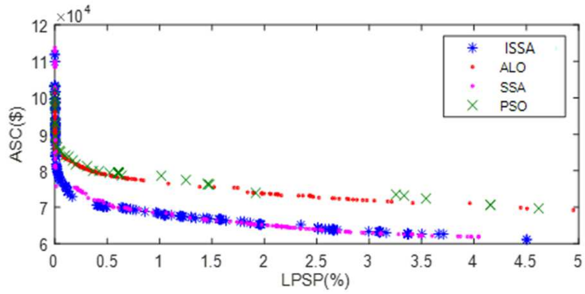

Fig. 5. Pareto plot of all four algorithms.

The depicted graph in Fig 6 illustrates the charge level in the storage system over three days. Analysis of the plot reveals that the state of charge (SOC) consistently remains under 30%, with the highest SOC recorded at 100%. In the daytime, surplus solar energy is stored in the battery system for later use, ensuring a continuous energy supply after sunset to meet demand. Consequently, the SOC of the battery system rises during daylight hours, peaking at 100%, and declines at night to meet energy requirements. Maintaining the SOC above the 30% threshold optimizes the design, prolonging the battery system's lifespan by preventing deep discharges.

BTS relies on available energy to meet its energy needs during operation. Fig 7, a graphical illustration, shows the utilization of HRES and BT to address load requirements. Solar and wind power are utilized daily to satisfy energy demands, with excess energy stored in batteries. Energy is then drawn from these batteries at night to meet load demands. In cases of inadequate energy storage, the DG system is activated. Fig 8 depicts the load demand for HRES and the BT system throughout one week. The yellow curve represents the surplus energy stored in the battery, which highlights that the battery remains fully charged in times of

TABLE II RESULTS COMPARISON OF ALL ALGORITHMS

Algo	Wind (kW)	PV size (kW)	Battery storage (kWh)	DG Size (kW)	LPSP (%)	COE ($/kWh)
ISSA	87.04	9.48	76.07	20.42	5	0.1521
PSO	96.58	1	91.56	15.40	5	0.1552
SSA	73.61	52.97	63.43	15.92	5	0.1538
ALO	72.43	34.56	64.16	23.37	5	0.1530

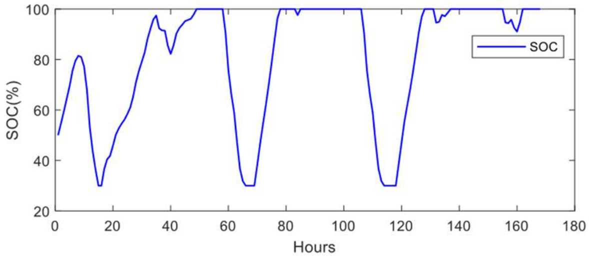

Fig. 6. Graph of SOC(%)of the battery storage system.

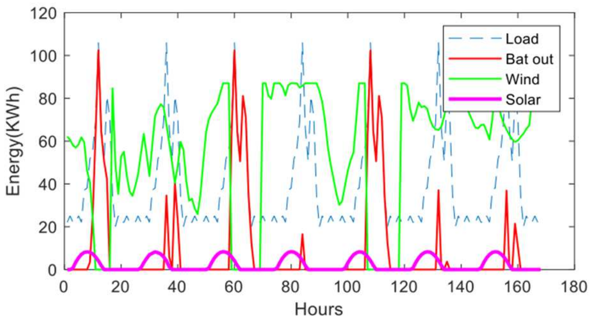

Fig. 7. The comparative plot of load demand, battery discharging wind and solar energy.

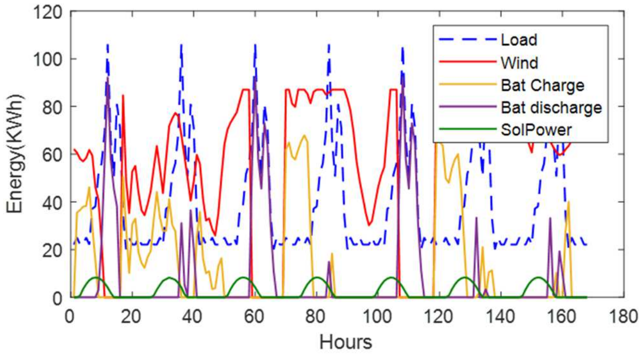

Fig. 8. Comparative representations of various factors including battery charging, load demand, battery discharging, wind energy, and solar energy

abundant renewable energy. In daylight hours, excess power is produced by the renewable energy system and stored in the battery storage system. Even with ample renewable energy around the 80th hour, the charging curve gradually diminishes to zero, indicating the battery's full charge status.

Fig 9 shows battery charging and discharging curves for the three days. The blue curve shows the charging curve of the battery storage system in case sufficient surplus renewable energy is available. The red curve shows the battery storage system's discharging during the night when solar energy is unavailable to fulfill the load demand. During the year, 97384.25 kWh of energy is stored in the battery storage system, which provides 87517.56 kWh of energy to the load.

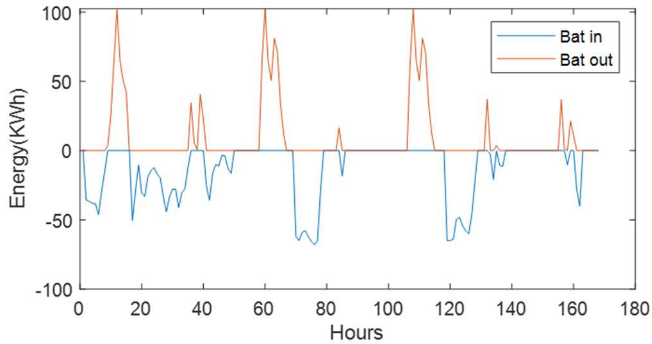

Fig. 9. Profile of battery charging and discharging.

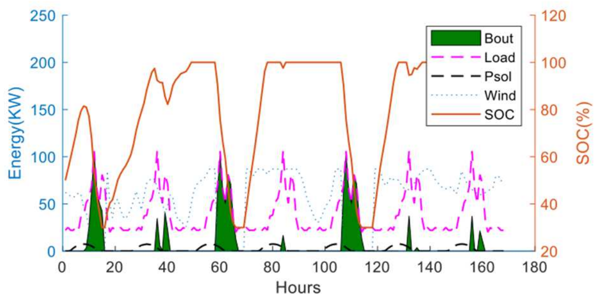

Fig 10. Graph of the generation and load balance, as well as the SOC of the BTS.

B. Comparison of Energy Generation with Load Demand and State of Charge

Gaining knowledge about the load requirements of Renewable Energy Sources (RES) and Battery Technologies (BT) in different day and night scenarios and creating effective plans to meet these load needs is crucial. Fig 10 visually compares energy generation, load demand, and battery storage system charge status. Wind and solar energy are suitable sources for charging the battery during the day, reducing the need for Diesel Generators (DG). However, when solar energy is unavailable, the BT system supplies power to the system. This highlights the importance of formulating a holistic approach to address the varying energy demands of a system. Additionally, an efficient battery storage system plays a significant role in promoting a sustainable energy environment by enhancing the utilization of RES.

Fig 11 demonstrates the monthly power generation, load demand, and annual battery charging-discharging. These diagrams offer insights into the mean wind energy generation, solar energy production, DG production, battery storage, and discharge, along with the load demand of the BTS. For instance, looking at January, it is evident that all of the load demand of the BTS is satisfied solely by solar and wind energy, without the DG needing to operate. However, in the summer season, especially during peak hours, the DG is employed to meet the increased load demand, as shown by the yellow bars in the diagrams.

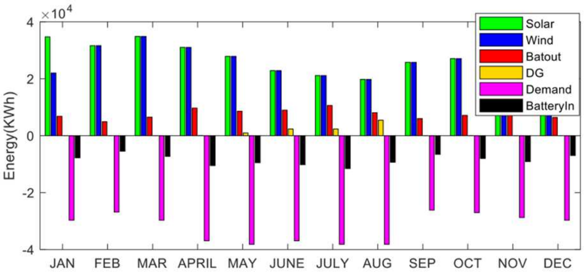

Fig 11. Power generation, load demand, and battery charging-discharging for the whole year.

V. CONCLUSIONS

The hybrid MOISSA algorithm delivered superior outcomes in contrast to other algorithms. The primary aim of this algorithm is to determine the best number of wind, PV, BT, and DG components while minimizing COE, and reducing LPSP. Moreover, the hybrid MOISSA algorithm has avoided premature convergence and eventually converges towards global optimal solutions. By offering more efficient and cost-effective solutions, the hybrid MOISSA algorithm in this study has contributed to the progress of RESs. A significant advantage of the hybrid MOISSA algorithm is its potential to produce highly accurate results that align with the research's stated goals. It is postulated that the algorithm's implementation in the study will enhance RESs by providing more effective solutions. This research evaluates the efficiency and effectiveness of the hybrid MOISSA algorithm in achieving the study's objectives.

The study's results demonstrate the hybrid algorithm's superiority over other algorithms. With a 0% LPSP, the hybrid MOISSA algorithm reaches the optimal design with a minimal COE of 0.2309$/kWh, in comparison to PSO, SSA, and ALO, which have COEs of 0.2856, 0.2726, and 0.2622 $/kWh, correspondingly. These findings demonstrate the superior performance of the hybrid algorithm over others. Similarly, with a 20% LPSP, the hybrid MOISSA algorithm exhibits the lowest COE of 0.1521$/kWh, while PSO, SSA, and ALO showcase COEs of 0.1552, 0.1538, and 0.1530$/kWh, respectively.

The Hybridized MOISSA algorithm has been employed to optimize a hybrid renewable energy system to fulfill the energy needs of a Base Transceiver Station (BTS) while considering various LPSP reliability limitations. A comparative analysis shows that this algorithm surpasses three other algorithms in terms of Cost of Energy (COE). The resulting optimized setup, which ensures a 20% LPSP, comprises a 101-kW wind turbine, a 42-kW PV system, an 80-unit battery storage system, and a small-scale DG. Therefore, the findings of this research indicate that the hybridized MOISSA algorithm demonstrates superior effectiveness in terms of the energy generation cost for an off-grid BTS.

REFERENCES

[1] Dalton, G. J., Lockington, D. A., & Baldock, T. E. (2009). Case study feasibility analysis of renewable energy supply options for small to medium-sized tourist accommodations. Renewable Energy, 34(4), 1134-1144.

[2] Gipe, P., & Möllerström, E. (2023). An overview of wind turbine development history: Part II–The 1970s onward. Wind Engineering, 47(1), 220-248.

[3] Chaudhari, M. S., & Tibude, S. A New Hybrid Solar-Wind Charging Station for Electric Vehicle Applications and Its Simulation.

[4] Ghorbani, N., Kasaeian, A., Toopshekan, A., Bahrami, L., & Maghami, A. (2018). I am optimizing a hybrid wind-PV battery system using GA-PSO and MOPSO to reduce cost and increase reliability. Energy, 154, 581-591.

[5] Ileana, Citaristi. (2022). United Nations Development Programme—UNDP. 183-188. doi: 10.4324/9781003292548-43.

[6] Zafar, M. A. B., Islam, M. R., Islam, M. S. U., Shafiullah, M., & Ikram, A. I. (2022, December). Economic analysis and optimal design of micro-grid using PSO algorithm. In 2022, the 12th International Conference on Electrical and Computer Engineering (ICECE) (pp. 421-424). IEEE.

[7] Ajlan, A., Tan, C. W., & Abdilahi, A. M. (2017). Assessment of environmental and economic perspectives for a renewable-based hybrid power system in Yemen. Renewable and Sustainable Energy Reviews, 75, 559-570.

[8] Sinha, S., & Chandel, S. S. (2014). Review of software tools for hybrid renewable energy systems. Renewable and sustainable energy reviews, 32, 192-205.

[9] Bernal-Agustín, J. L., & Dufo-Lopez, R. (2009). Simulation and optimization of stand-alone hybrid renewable energy systems. Renewable and sustainable energy reviews, 13(8), 2111-2118.

[10] Al Garni, H. Z., Mas' ud, A. A., & Wright, D. (2021). Design and economic assessment of alternative renewable energy systems using capital cost projections: a case study for Saudi Arabia. Sustainable Energy Technologies and Assessments, 48, 101675.

[11] Fathy, A., Kaaniche, K., & Alanazi, T. M. (2020). A recent approach-based social spider optimizer for optimal sizing hybrid PV/wind/battery/diesel integrated microgrid in Aljouf region. IEEE Access, 8, 57630-57645.

[12] Farh, H. M., Al-Shamma'a, A. A., Al-Shaalan, A. M., Alkuhayli, A., Noman, A. M., & Kandil, T. (2022). Technical and economic evaluation for off-grid hybrid renewable energy system using novel bonobo optimizer. Sustainability, 14(3), 1533.

[13] Jufri, F. H., Aryani, D. R., Garniwa, I., & Sudiarto, B. (2021). Optimal battery energy storage dispatch strategy for small-scale isolated hybrid renewable energy system with different load profile patterns. Energies, 14(11), 3139.

[14] Borhanazad, H., Mekhilef, S., Ganapathy, V. G., Modiri-Delshad, M., & Mirtaheri, A. (2014). Optimization of micro-grid system using MOPSO. Renewable energy, 71, 295-306.

[15] Sinha, S., & Chandel, S. S. (2015). Review recent trends in optimization techniques for solar photovoltaic–wind-based hybrid energy systems. Renewable and sustainable energy reviews, 50, 755-769.

[16] Anoune, K., Bouya, M., Astito, A., & Abdellah, A. B. (2018). Sizing methods and optimization techniques for PV-wind based hybrid renewable energy system: A review. Renewable and Sustainable Energy Reviews, 93, 652-673.

[17] Bashir, N., Modu, B., & Harcourt, P. (2018). Techo-economic analysis of off-grid renewable energy systems for rural electrification in North-eastern Nigeria.

[18] Seedahmed, M. M., Ramli, M. A., Bouchekara, H. R., Milyani, A. H., Rawa, M., Budiman, F. N., ... & Hassan, S. M. U. (2022). Optimal sizing of a grid-connected photovoltaic system for a large commercial load in Saudi Arabia. Alexandria Engineering Journal, 61(8), 6523-6540.

[19] Thirunavukkarasu, M., & Sawle, Y. (2021). A comparative study of the optimal sizing and management of off-grid solar/wind/diesel and battery energy systems for remote areas. Frontiers in Energy Research, 9, 752043.

[20] Omar, A. S., Mohamed, A. A. A., Senjyu, T., & Hemeida, A. M. (2019, October). Multi-Objective Optimization of a Stand-alone Hybrid PV/wind/battery/diesel Micro-grid. In 2019 IEEE Conference on Power Electronics and Renewable Energy (CPERE) (pp. 391-396). IEEE.

[21] Zhu, W., Guo, J., Zhao, G., & Zeng, B. (2020). Optimal sizing of an island hybrid microgrid based on improved multi-objective grey wolf optimizer. Processes, 8(12), 1581.

[22] Wang, J., Gao, Y., & Chen, X. (2018). A novel hybrid interval prediction approach based on modified lower upper bound estimation in combination with multi-objective salp swarm algorithm for short-term load forecasting. Energies, 11(6), 1561.

[23] Wang, J., Gao, Y., & Chen, X. (2018). A novel hybrid interval prediction approach based on modified lower upper bound estimation in combination with multi-objective salp swarm algorithm for short-term load forecasting. Energies, 11(6), 1561.

[24] Duan, Q., Wang, L., Kang, H., Shen, Y., Sun, X., & Chen, Q. (2021). It improved the salp swarm algorithm with simulated annealing for solving engineering optimization problems: symmetry, 13(6), 1092.

[25] Balakrishnan, K., Dhanalakshmi, R., & Khaire, U. M. (2021). Improved salp swarm algorithm based on the levy flight for feature selection. The Journal of Supercomputing, 77(11), 12399-12419.

[26] Wang, J., Gao, Y., & Chen, X. (2018). A novel hybrid interval prediction approach based on modified lower upper bound estimation in combination with multi-objective salp swarm algorithm for short-term load forecasting. Energies, 11(6), 1561.

[27] Abualigah, L., Shehab, M., Alshinwan, M., & Alabool, H. (2020). Salp swarm algorithm: a comprehensive survey. Neural Computing and Applications, 32(15), 11195-11215.

[28] Yadong, W., & Weixing, S. (2019, June). Improve Multi-objective Ant Lion Optimizer Based on Quasi-oppositional and Levy Fly. In 2019 Chinese Control and Decision Conference (CCDC) (pp. 12-17). IEEE.